J. Exp. Path. (1990), 71, 411–422

Anti-glomerular basement membrane (GBM) glomerulonephritis in the mouse: development of disease and cell proliferation

Janice Wheeler,* A.R. Morley† and D.R. Appleton‡
*Departments of *Microbiology, †Histopathology and ‡Medical Statistics, University of Newcastle upon Tyne, UK*

Received for publication 30 October 1989
Accepted for publication 15 January 1990

Summary. In a mouse model of anti-glomerular basement membrane (GBM) glomerulonephritis, associated with the nephrotic syndrome, a wide range of morphological and proliferative responses was seen in the renal corpuscle, at 6 days. The severity of the damage could be assessed by measuring the average daily weight gain between days 0 and 3 (DWG) of the animal. Those animals with a high DWG showed capsular proliferation, whereas animals with a low DWG showed predominantly tuft cell proliferation. Capsular cell birth rate increased with DWG whilst tuft cell birth rate was negatively related. A computer simulation suggests that the results are compatible with the induction of successive but overlapping waves of tuft and capsular cell proliferation.

Keywords: anti-GBM, glomerulonephritis, mitotic indices, mouse, simulation, vincristine

Crescentic glomerulonephritis is an important cause of renal failure. Crescent formation follows severe glomerular damage, irrespective of the underlying immune mechanism, and the prognosis for renal function is closely related to the percentage of renal corpuscles damaged or destroyed and, thus, to the extent of glomerular occlusion (Zollinger & Mihatsch 1978).

Many studies of crescentic glomerulonephritis, in man and experimental animals, have indicated that both proliferation and accumulation of cells in Bowman's capsule play some part in crescent development. However, there have been very few quantitative cell proliferation studies other than those of Sterzel and Pabst in the rat (Sterzel & Pabst 1982; Pabst & Sterzel 1983) and Cattell and Jamieson (1978) in the rabbit. Powerful cell kinetic methods, such as the fraction labelled mitoses method, are available for the measurement of cell cycle parameters but have not been used in the study of glomerulonephritis. Three major factors are perhaps responsible:

(i) the requirement for a reproducible model of crescentic glomerulonephritis in an animal small enough to enable a cell kinetic study to be practical and financially viable;
(ii) the overall cellular and morphological complexity of the renal corpuscle
(iii) the low rate of proliferation in the renal corpuscle cells.

In 1985, we published a model of crescentic glomerulonephritis in T70 (Beige) mice (Morley & Wheeler 1985), which was

Correspondence: Dr Janice Wheeler, Department of Microbiology, University of Newcastle upon Tyne, The Medical School, Framlington Place, Newcastle upon Tyne NE2 4HH, UK.

induced by preimmunization with rabbit IgG and subsequent immunization with four injections of rabbit anti-mouse glomerular basement membrane (GBM) antiserum (total dose 0.4 ml). The glomerulonephritis was characterized by a linear deposition of rabbit IgG on the GBM, the deposition of fibrin in the glomerular tuft and proliferation of cells in Bowman's capsule. Crescents were visible in some renal corpuscles within 11 days of the final injection.

Further studies in this laboratory showed that the onset and course of the disease were accelerated by increasing the total dose of antiserum administered to 0.8 ml. With this protocol, extensive glomerular damage was evident in some animals within 6 days, although inter-animal variation was apparent. The onset and severity of the lesion, however, could be followed with a high degree of accuracy by measuring the daily weight gain which was associated with oedema, ascites, and deposition of fibrin in the glomerular tuft.

In this paper, we report the results of a series of experiments with this accelerated model, using consecutive bleeds of antiserum from a single rabbit. We examine the factors influencing the onset and course of the glomerulonephritis and associated changes in the biochemistry, morphology and cell proliferation in the renal corpuscle.

Materials and methods

Experimental animals

Inbred T70 (Beige) mice [$(C3H^{*}101)F_1$ hybrids] were originally obtained from the MRC Radiobiology Unit, Harwell, Didcot, Oxon and were then maintained by continuous brother–sister mating.

One New Zealand White male rabbit was purchased from Ranch Rabbits (Crawley Down, Sussex).

All animals were housed in the Comparative Biology Centre of the University of Newcastle upon Tyne and had unrestricted access to food and water.

Preparation of mouse glomerular basement membranes (GBM)

Lyophilized GBM was obtained from normal mouse kidneys, as detailed previously (Morley & Wheeler 1985) and stored at −30°C.

Production of rabbit anti-mouse GBM antiserum

One New Zealand White male rabbit was immunized with five intramuscular injections of 10 mg of lyophilized mouse GBM, given over a period of 30 days. The antigen was administered as a water-in-oil-in-water (w.o.w) emulsion in Freund's adjuvant (Freund's Complete Adjuvant (FCA) for the first injection and Freund's Incomplete Adjuvant (FIA) for the remaining injections). Booster injections of 10 mg (approximately) of mouse GBM were then given, at intervals of approximately 2 months. The rabbit was bled from the marginal vein 10–14 days after each boost and the serum obtained was stored at −20°C. The anti-GBM titre of each bleed was determined by a modification of the ELISA of Wheeler *et al.* (1988).

Eight consecutive bleeds, obtained approximately 13–28 months after the initial injection of GBM, were used in this study. All eight sera had similar high levels of circulating anti-mouse GBM antibodies.

Experimental design for the induction of anti-GBM glomerulonephritis

T70 (Beige) male mice, of known age and weight, were pre-immunized by a subcutaneous injection of a w.o.w. emulsion of 0.33 mg rabbit IgG (Nordic Immunological Reagents, Berks) in FCA, on day −4. On days −3, −2, −1 and 0, alternate intravenous/intraperitoneal injections of rabbit anti-mouse GBM antiserum were administered (0.1 ml i.v./0.3 ml i.p.).

Control groups of mice, matched for age and weight, were also used in early experiments. These animals were immunized with rabbit IgG on day −4, but were then given,

on days −3, −2, −1, and 0, alternate i.v./i.p. injections of phosphate-buffered saline (PBS) pH 7.4.

Mice were weighed daily and carefully monitored for evidence of oedema and haematuria. Prior to sacrifice on day 6, some mice were used for in-vivo stathmokinetic experiments, as detailed below.

Mice were killed by cervical dislocation and kidneys were removed and fixed in formal saline for examination by light microscopy. Wherever possible, serum and urine samples were also obtained for biochemical measurements.

In-vivo stathmokinetic experiments

In order to evaluate cellular proliferation, mitotic arrest experiments were performed with the stathmokinetic drug, vincristine, which blocks mitosis at metaphase.

Mice were injected intraperitoneally with 30 μg of vincristine sulphate per kg body weight. The animals were then killed by cervical dislocation at intervals thereafter, for up to 3.5 hours. Kidneys, serum and urine were obtained and treated as detailed previously.

Light microscopy

Tissues fixed in formal saline were dehydrated through a graded series of alcohols, cleared in xylene, and impregnated with paraffin wax. Sections at 2 μm were stained with haematoxylin and eosin (H/E) and periodic acid–Schiff (PAS).

Glomerular measurements

To obtain estimates of mitotic indices in the glomerular tuft and in Bowman's capsule, 1000 tuft or capsular cells were counted and the number of mitoses in these 1000 cells expressed as a percentage. All glomerular measurements were performed on coded slides to avoid observer bias.

Biochemical measurements

Serum urea and cholesterol levels and urinary protein concentrations were measured by the Department of Clinical Biochemistry, Royal Victoria Infirmary, Newcastle upon Tyne.

Statistical methods

Linear regression, Spearman rank correlation (r_S) and *t*-tests on logarithmically transformed data were used as detailed.

Results

Induction of glomerulonephritis

Eight experiments, using a total of 99 test mice, 25 controls and rabbit anti-mouse GBM antiserum from eight consecutive bleeds, were carried out according to the protocol outlined in Materials and methods (Table 1). The approximate weight and age ranges of the animals were 17–34 g and 5–21 weeks.

Full daily weight data were obtained from seven experiments, involving 88 test mice and 14 controls. The average daily weight gain between days 0 and 3 (DWG) was estimated for each of these animals by linear regression.

As can be seen from Table 1 and Fig. 1, there was a considerable variation in the responses of the test mice to the injection regime in all seven experiments, with DWG ranging from 0 to 3.25 g/day. In contrast, the DWG of the control animals ranged from −0.43 to 0.23 g/day.

Some test animals showed a rapid gain in weight following injection. This was associated with general inactivity and swelling of the abdomen, which was shown, at subsequent autopsy on day 6, to be the result of ascites and tissue oedema. Haematuria was often evident by days 5–6. The kidneys in such animals were observed, at autopsy, to be enlarged and paler than those of control mice.

Table 1. Daily weight gain (DWG) in glomerulonephritic and control T70 (Beige) mice; experiments 1–8

Expt	Antiserum bleed number	Glomerulonephritic mice		Control mice	
		n	DWG (g/day) ($\bar{x}\pm$s.d.)	*n*	DWG (g/day) ($\bar{x}\pm$s.d.)
1	7	11	—	11	—
2	8	5	1.04±0.39	4	0.01±0.09
3	9	7	1.60±0.71	10	−0.05±0.21
4	10	15	1.68±0.46		
5	11	10	0.29±0.13		
6	11	25	1.71±0.84		
7	12/13/14 pool	10	0.30±0.15		
8	12/13/14 pool	16	0.80±0.72		

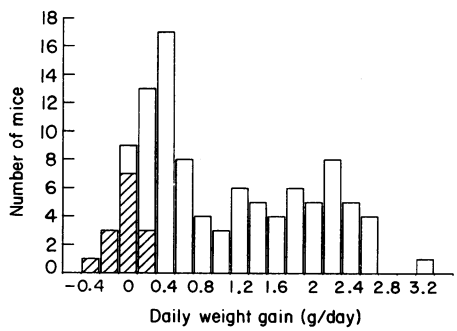

Fig. 1. Histogram of daily weight gains in □, glomerulonephritic ($n=88$) and ▨, control ($n=14$) T70 (Beige) mice.

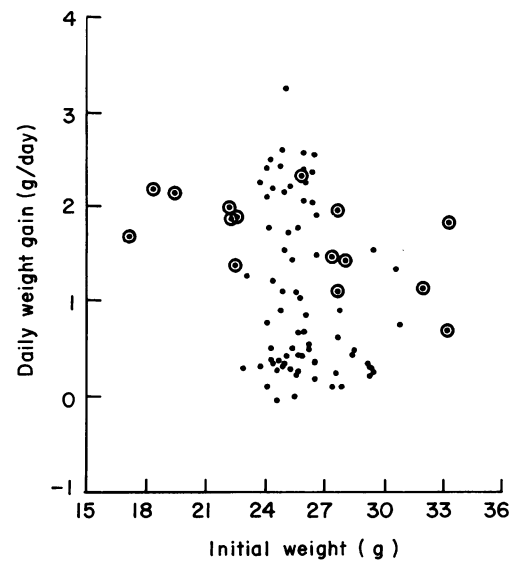

Fig. 2. Relationship between daily weight gain and initial weight in glomerulonephritic mice ($n=88$). Results from Experiment 4 are represented as ⊙.

In contrast, other test mice showed a much slower gain in weight. These animals remained active over this period, with no obvious oedema, ascites or haematuria. At autopsy on day 6, the kidneys of these animals were the same size and colour as those from control animals.

Rank correlation analysis of the daily weight gain data of the test animals for each individual experiment showed no correlation with either the initial weights or ages of the mice, with the exception of Experiment 4. The combined results of DWG against initial weight for all seven experiments are shown in Fig. 2, highlighting the results of Experiment 4. In this particular experiment, 15 mice, ranging from 17 to 34 g and from 5 to 16 weeks, were used. The results suggest that lighter and younger animals show a greater daily weight gain, but the relationships are of low significance ($P=0.038$ for weight; $P=0.012$ for age). As weight is highly correlated with age, it is not possible to separate the effects of age and weight on daily weight gain.

Using the whole series (88 cases), Spearman rank correlation confirms a highly significant relationship between age and weight ($r_S = 0.525$) and significant negative correlations between DWG and age ($r_S = -0.352$; $P = 0.0026$) and weight ($r_S = -0.245$; $P = 0.022$).

Morphological studies

No evidence of abnormality was found in any of the control animals. However, in the test mice, microscopy revealed that glomerular and tubular abnormalities appeared to be related to the weight changes of the animals.

The morphological changes seen in mice with a high DWG were much greater than those seen in mice with a low DWG, although there was often considerable variation within a single kidney. In the more severely damaged renal corpuscles (Fig. 3a), there were heavy deposits of hyaline material in the glomerular capillary loops, often extending into the afferent arterioles. Electron microscopy showed this material to have the characteristic cross-banding of fibrin. Vacuolation of podocytes was also evident and there were considerable amounts of protein in the tubular cytoplasm. Observations suggested that there was a relationship between the amount of fibrin in the glomerular tuft and mitotic activity in Bowman's capsule, although early crescent formation was only occasionally seen. These changes were particularly marked in the large renal corpuscles close to the medulla. Mitotic activity in the capillary loops of the tuft was rare in such animals.

Morphological studies on day 6 in mice with low DWG indicated only an increased cellularity of the glomerular tuft, in which polymorphs were uncommon (Fig. 3b). Mitotic figures were seen in the glomerular tuft but rarely in Bowman's capsule. Tubular changes were also less pronounced than in animals with high DWG, comprising hyaline drops in the straight part of the proximal convoluted tubule.

Biochemical studies

Urinary protein was measured throughout the course of Experiment 4, samples being obtained daily from as many of the 15 mice as possible. The results are illustrated in Fig. 4 against those from 12 control animals and show that, in all test mice, by day 3, proteinuria was greatly increased above the normal range.

Serum urea levels were measured, on day 6, in six test mice and 13 controls, throughout the series of experiments. The results are shown in Fig. 5a and illustrate that, in all cases, the serum urea levels of the test mice were well above the normal range. However, the small positive correlation with DWG was not significant ($P = 0.26$; log-transformed t-test).

Serum cholesterol levels were also measured, on day 6, in 10 test animals and four controls (Fig. 5b). As with urea, the cholesterol levels of all test animals were above the normal range. Furthermore, these results indicated that those mice exhibiting the higher DWG showed the largest increase in serum cholesterol ($P = 0.0001$; log-transformed t-test), though this finding depends crucially on the three mice with very high DWG.

In-vivo stathmokinetic experiments

Vincristine mitotic arrest. Observations in morphological studies had strongly suggested an inverse association between capsular and tuft cell proliferation in renal corpuscles. To investigate this more fully, the vincristine mitotic indices, in Bowman's capsule and the glomerular tuft, were measured on day 6 in 22 test mice, 120 min after the administration of 30 μg vincristine sulphate.

The results of the mitotic index in Bowman's capsule against DWG are shown in Fig. 6a and illustrate that, in general, the capsular mitotic index was higher in animals with a high DWG than with a low DWG. In contrast, the mitotic index in the glomerular tuft was higher in mice with a low DWG than

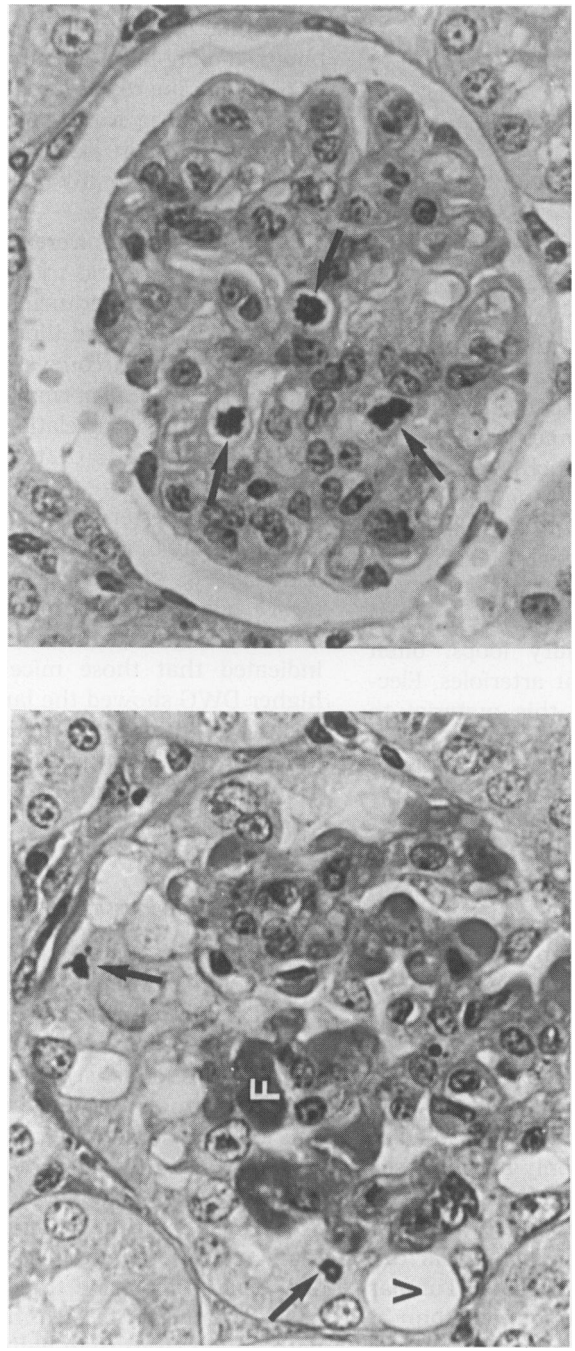

Fig. 3 a, Appearance on day 6 of renal corpuscle from mouse with high daily weight gain, showing fibrin (F), vacuolation (V) and mitoses (↑) in Bowman's capsule. PAS: final magnification × 800. b, Appearance on day 6 of renal corpuscle from mouse with low daily weight gain, showing hypercellular glomerular tuft with intra-tuft mitoses (↑) PAS: final magnification × 800.

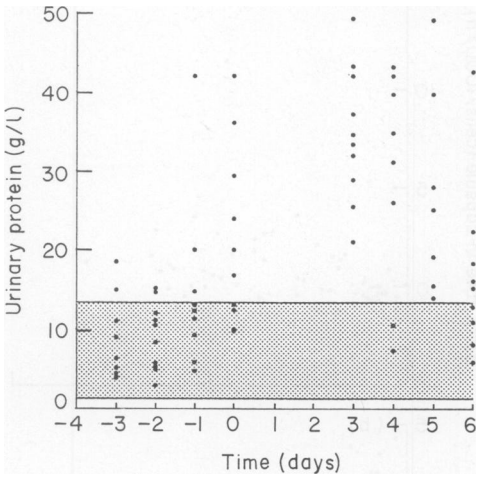

Fig. 4. Development of proteinuria during experimental anti-GBM glomerulonephritis in T70 (Beige) mice. ▨, 95% range.

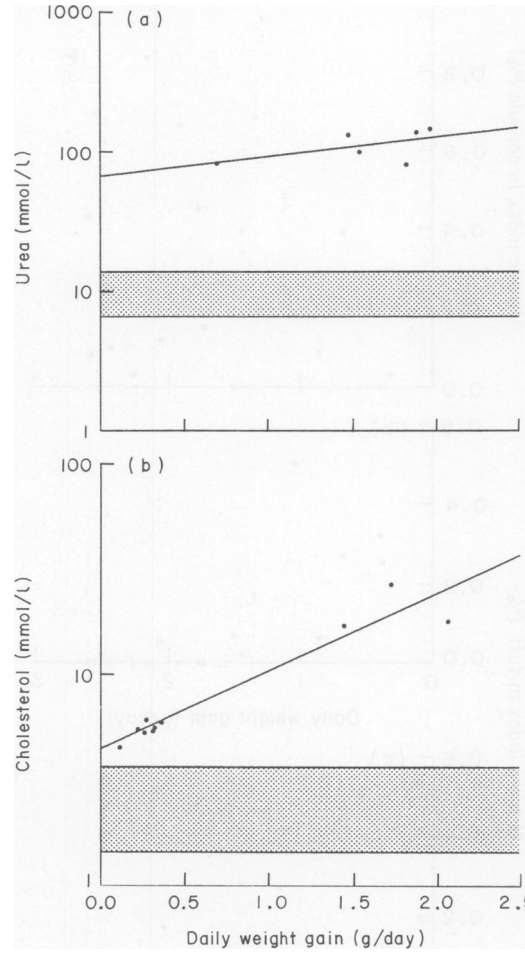

Fig. 5. Relationship between daily weight gain and a, serum urea and b, serum cholesterol in glomerulonephritic T70 (Beige) mice. ▨, 95% range.

with a high DWG (Fig. 6b). The inverse relationship between capsular and tuft cell proliferation is clearly illustrated in Fig. 6c.

Cell birth rate studies. The daily weight gain reflects functional damage to the glomerular basement membrane, whereas the mitotic indices are measures of the cellular response to immunological events within the renal corpuscle. It is, therefore, of interest to examine the relationship between daily weight gain and cell birth rate in the glomerular tuft and the capsule.

Assuming a constant increase in mitotic index with time after vincristine, the birth rate of cells can be calculated from the vincristine arrest data as follows:

$$\text{Birth rate} = \{MI(t) - MI(t=0)\}/(t/60)$$
$$= \text{cells}/1000 \text{ cells/h}$$

where MI = mitoses/1000 cells and t = duration of vincristine treatment (min)

The capsular and tuft mitotic indices on day 6 were measured in 69 test mice at various time intervals up to 200 min after administration of 30 μg vincristine sulphate. The mitotic indices at time zero were estimated from four test mice, which were not given vincristine.

In the test animals, the results of cell birth rate in the capsule against DWG show that the birth rate increased slowly but significantly with increasing DWG (Fig. 7a: $r_S = 0.473$; $P = 0.0001$). Conversely, the tuft cell birth rate diminished with DWG (Fig. 7b:

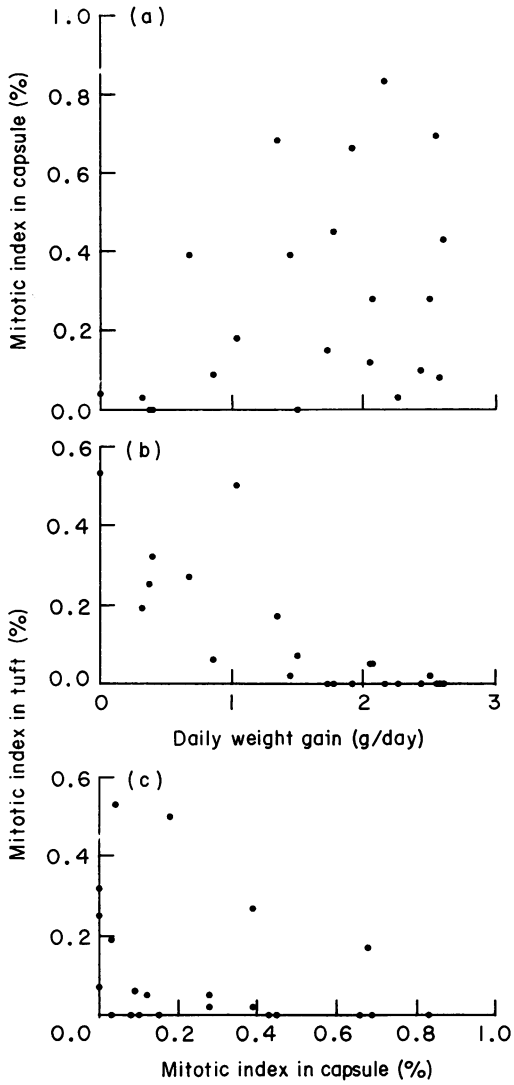

Fig. 6. Relationship between daily weight gain and mitotic indices in a, capsule and b, tuft on day 6, 120 min after administration of vincristine. c, Relationship between capsular and tuft mitotic indices on day 6, 120 min after administration of vincristine.

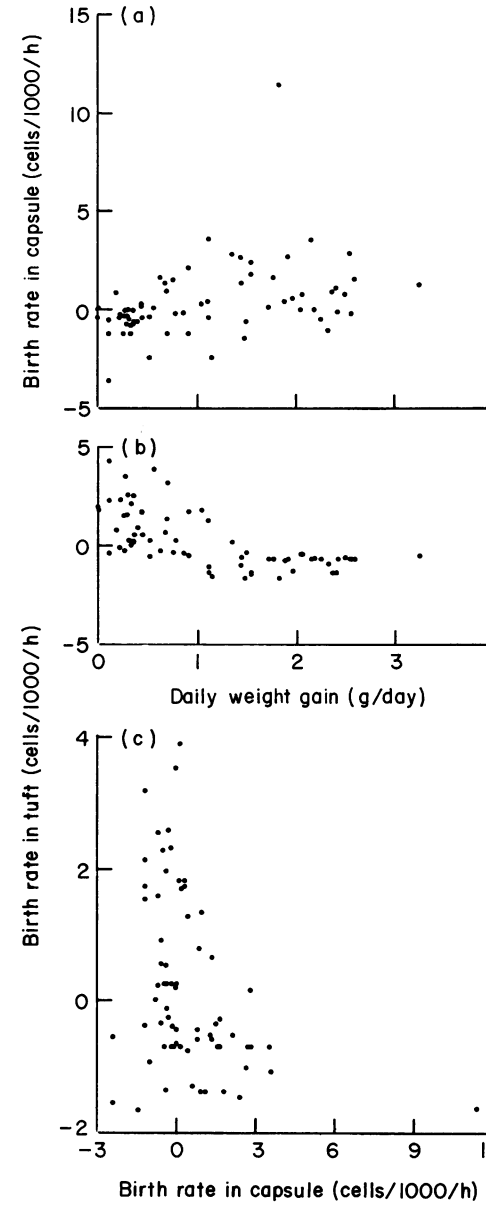

Fig. 7. Relationship between daily weight gain and a, capsular and b, tuft birth rates, measured on day 6. c, Relationship between capsular and tuft birth rates, measured on day 6.

$r_S = -0.734$; $P = 0.0001$). Histological examination had suggested that mitotic activity in the tuft was not usually found at the same time as capsular proliferation. These results support this observation (Fig. 7c). Analysis shows a significant negative relationship between the two birthrates ($r_S = -0.393$; $P = 0.0012$).

Discussion

Glomerulonephritis has been produced in both rat models (Dubois *et al.* 1981; Silva *et al.* 1984; Foellmer *et al.* 1986) and mouse models (Nagai *et al.* 1985; Schrijver *et al.* 1989), after treatment with heterologous anti-GBM antibodies. Whilst this study confirms the usefulness of such mouse models, it also highlights the problems of inter-animal variability, as a wide range of responses was found. However, the onset and severity of the renal lesion in this mouse model was successfully monitored by measuring the daily weight gain in the 3 days following the last injection. This parameter, therefore, serves as a useful in-vivo guide to the severity of the renal lesion.

Several factors appear to contribute to the variability of response seen in this series of experiments. Negative correlations were found between DWG and both the initial weights and ages of the animals, the relationship with age being the more significant. However, because of the high correlation between weight and age in growing animals, the importance of either factor alone cannot be determined. The relationship with weight may have reflected a dose response, whilst the relationship with age suggests that younger animals are more susceptible to glomerular damage. The latter may be partly accounted for by the observation that the development of the male mouse capsular epithelium is age-related, occuring at 5 to 10 weeks (Hamada 1979).

The use of consecutive bleeds of antiserum from the same rabbit must also be considered as a possible source of inter-experimental variability. Although there were no significant differences in the anti-GBM antibody titres of the eight bleeds used, the proportions and affinities of the various antibody populations within each bleed may have differed.

Whilst the above factors appear to contribute to the observed variability of response, it seems likely that the individual animal response is a major factor in the development of glomerular damage.

A prominent feature of the previously mentioned rat and mouse models of glomerulonephritis is the development of proteinuria. This study confirms this finding, as all test animals showed urinary protein levels above the physiological proteinuria found in the mouse. Furthermore, the tissue oedema and ascites seen in this model are due to the development of nephrotic syndrome, indicated by the increased serum levels of both urea and cholesterol. It is interesting that the development of severe proteinuria and features of nephrotic syndrome are rarely seen in anti-GBM disease in man.

A feature particularly noted in those mice showing a high DWG was the presence of large vacuoles, apparently within podocytes. These structures have recently been studied by Furness *et al.* (1989), who have described two types of balloon-like swellings, both associated with proteinuria. In the first, there is formation of a space between a podocyte and the glomerular basement membrane, with loss of the epithelium from the basement membrane. This type appears confined to nephropathy produced by puromycin aminonucleoside. In the second type, the vacuole is bounded on all sides by podocyte epithelium and occurs in a range of experimental nephritides associated with proteinuria. It is suggested that the sub-epithelial accumulation of fluid results from damage to the podocytes.

Morphological observations indicated that an early change was an increased cellularity of the glomerular tuft, in which polymorphonuclear leucocytes were uncommon. This finding contradicts the observations of Schrijver *et al.* (1989), who reported a glomerular influx of such cells in a Beige mouse model of anti-GBM disease. However, since Schrijver's observations were made 2–24 h after the injection of rabbit anti-mouse GBM antibodies and our observations were confined to day 6, it is possible that a short-lived accumulation of polymorphs had been missed. Schrijver *et al.* (1989) further showed that the induction of proteinuria and glomerular lesions could be prevented by

depletion of polymorphs and that the polymorph neutral proteinases were responsible for the proteinuria. Other studies, however, have reported mononuclear cell infiltration (monocytes and macrophages) in the early phases of response to heterologous antibodies (Dubois *et al.* 1981; Foellmer *et al.* 1986).

The features of glomerulonephritis described in this model show considerable similarity to the immune complex mouse model of Sawtell *et al.* (1987). i.e. heavy proteinuria accompanying massive ascites and early crescent formation. Another feature common to both models is the presence of intracapillary deposits of fibrin in the early stages of the lesions. The rat anti-GBM model of Silva *et al.* (1984) also features tuft fibrin deposition, although, in this case, large amounts of fibrin-related antigens were also detected in Bowman's space, coincident with crescent formation. This feature, which is similar to the appearance in man, was not observed in our mouse model, but this discrepancy may again be explained by the timing of our observations.

Our attempts to demonstrate cell proliferation with vincristine-induced mitotic arrest indicated that the tuft and Bowman's capsule were showing different cell kinetic behaviour, in that inverse association between tuft and capsular proliferation was demonstrated. Since tuft proliferation was seen mainly in mice showing a low DWG, this suggested that tuft proliferation precedes capsular proliferation. This finding is consistent with the observations of Sterzel and Pabst (1982), who studied both mitotic indices and tritiated thymidine labelling indices in a rat model of glomerulonephritis.

This suggestion that tuft mitotic activity precedes that in the capsule is difficult to test in a longitudinal study in this animal model, since only one sample point per mouse can be obtained and there is considerable inter-animal variation. We have, therefore, undertaken a computer simulation, in which populations of tuft cells and then capsular cells undergo sequential waves of mitosis, with some degree of variation in the rates at which these events occur (see Appendix for description). A realization of the simulated waves of mitosis in the tuft and capsule is shown in Figs 8a and b respectively. Figure 8c demonstrates the relationship between the tuft and capsular mitotic indices, when they are sampled at a single point in time, midway between the two waves of mitotic activity. There is considerable similarity between the simulated relationship and that demonstrated in our mouse model (Fig. 6c). Whilst we have no data on the general shape of the waves of mitotic activity in our experimental animals, the use of this simulation demonstrates that our results are compatible with the hypothesis of a wave of tuft mitotic activity followed by a similar wave in the capsular epithelium. Furthermore, simulation excludes two other possibilities: that the waves of mitotic activity are close together in time, or that the waves are completely separate. The association of these two waves of mitotic activity in time does not, however, prove any causal relationship.

Although the cell birth rates in both tuft and capsule in this model were measured, we have no corresponding information on the rates of cell death or cell loss from the renal corpuscle. Our observation of the formation of crescentic structures in Bowman's capsule suggests that, in the capsule, there must have been a net excess of cells produced. In the glomerular tuft, however, there was little residual evidence of the observed proliferation. These estimates assume that all renal corpuscles are in a similar state of proliferative readiness. Counting a large sample may include glomeruli in which there is no significant damage and in which the cells have not entered the cell cycle (i.e. G_0 cells). This is equivalent to saying that the cells have a low growth fraction. Present studies are scanty (Litvak & Baserga 1964) but suggest that, as in the liver (Choie & Richter 1978) many renal epithelial cells are in G_0 (resting phase), but are capable of proliferation after an appropriate trigger. Since the development of crescents, in both man and

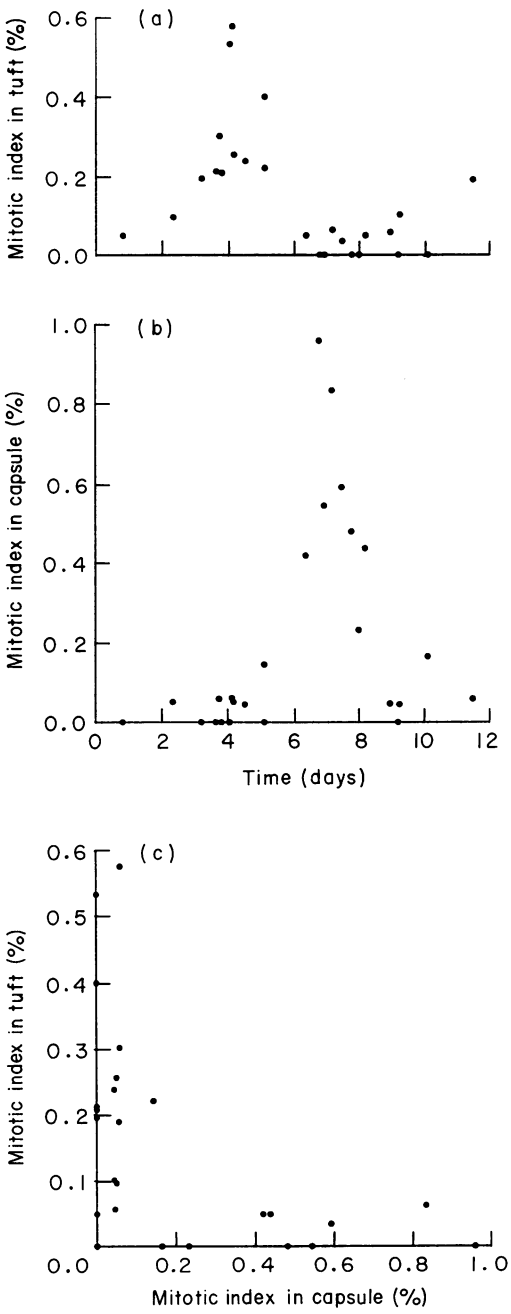

Fig. 8. Computer simulated waves of mitotic activity in a, tuft and b, capsule, separated by 5 days. c, Relationship between computer simulated mitotic indices in tuft and capsule. The values of the parameters which give rise to the results in Fig. 8 are:

$t_1^T = 2$ days $\quad t_1^C = 5$ days
$t_2^T = 4$ days $\quad t_2^C = 7$ days
$t_3^T = 6$ days $\quad t_3^C = 9$ days
$u_n = 2000 \quad t_{obs} = 6$ days
$o_n = 200 \quad o_{obs} = 2.5$ days
$IM_{native} = 0.05\%$
$IM_{max}^T = 0.40\%$
$IM_{max}^C = 0.70\%$

experimental animals, can occur alongside apparently normal renal corpuscles, it seems probable that there is variation in the susceptibility of individual renal corpuscles to the triggering stimulus or in the strength of the stimulus at the corpuscular level.

Further longitudinal studies are, therefore, required to determine the detailed changes in the tuft and capsular cell proliferation. These should be combined with an examination of the distribution and severity of the glomerular lesion within individual kidneys.

Acknowledgements

We are indebted to the Northern Counties Kidney Research Fund and the District Research Committee of Newcastle Health Authority for financial support. We also thank Mrs Linda Wragg and Mrs Susan Stamp for technical assistance.

Appendix

Computer simulation of sequential waves of mitotic activity in the glomerular tuft and capsule

A simple model was built in which the mitotic index in both tuft and capsule is at a low level IM_{native}, until at time t_1^T it begins to rise linearly in the tuft to a maximum level IM_{max}^T at time t_2^T, from which it immediately falls, again linearly, to reach its original level

at time t_3^T. At some time t_1^C (after t_1^T) the capsule similarly rises to a maximum mitotic index IM_{max}^C at time t_2^C and then falls to IM_{native} at t_3^C.

It is assumed that n animals are studied and that the numbers of mitoses seen in the tuft and capsule of each are random Poisson variables from distributions whose means depend on the mitotic indices calculated from the model described above and the numbers of cells counted; this is taken to be a random variable distributed uniformly (mean u_n: standard deviation o_n) over a range compatible with the numbers of cells counted in the experiments. The times at which these measurements are made are random normal variates, with mean t_{obs} and standard deviation o_{obs}, such that nearly all lie between t_1^T and t_3^C. In the actual experiments, all the measurements were made on the same day, but the times of response varied from animal to animal; we model this by having no inter-animal variation in time of response, but introducing the variability by changing the time of measurement.

References

CATTELL V. & JAMIESON S.W. (1978) The origin of glomerular crescents in experimental nephrotoxic serum nephritis in the rabbit. *Lab. Invest.* 39, 584–590.

CHOIE D.D. & RICHTER G.W. (1978) G2 subpopulation in mouse liver induced into mitosis by lead acetate. *Cell Tissue Kinet.* 11, 235–239.

DUBOIS C.H., FOIDART J.B., HAUTIER M.B., DECHENNE C.A., LEMAIRE M.J. & MAHIEU P.R. (1981) Proliferative glomerulonephritis in rats: evidence that mononuclear phagocytes infiltrating the glomeruli stimulate the proliferation of endothelial and mesangial cells. *Eur. J. Clin. Invest.* 11, 91–104.

FOELLMER H.G., STERZEL R.B. & KASHGARIAN M. (1986) Progressive glomerular sclerosis in experimental antiglomerular basement membrane glomerulonephritis. *Am. J. Kidney Dis.* 7, 5–11.

FURNESS P.N., TURNER S.N., APPLEBY P. & TURNER D.R. (1989) A morphological study of experimental proteinuria using a novel form of surface fixation. *J. Pathol.* 157, 37–46.

HAMADA Y. (1979) Sex difference and fine structure on epithelium cells of Bowman's capsule in mice (author's translation). *Jikken Dobutsu* 28, 485–490.

LITVAK R.M. & BASERGA R. (1964) An autoradiographic study of the uptake of ^{3}H-thymidine by kidney cells of mice at different ages. *Exp. Cell Res.* 33, 540–552.

MORLEY A.R. & WHEELER J. (1985) Cell proliferation within Bowman's capsule in mice. *J. Pathol.* 145, 315–327.

NAGAI H., YAMADA H., NISHIGAKI T., NAKAZAWA M. & KODA A. (1985) The susceptibility of experimental glomerulonephritis in six different strains of mice. *J. Pharmacobio-Dyn.* 8, 586–589.

PABST R. & STERZEL R.B. (1983) Cell renewal of glomerular cell types in normal rats. An autoradiographic analysis. *Kidney Int.* 24, 626–631.

SAWTELL N.M., WEISS M.A., PESCE A.J. & MICHAEL J.G. (1987) An immune complex glomerulopathy associated with glomerular capillary thrombosis in the laboratory mouse: A highly reproducible accelerated model utilizing cationized antigen. *Lab. Invest.* 56, 256–263.

SCHRIJVER G., SCHALKWIJK J., ROBBEN J.C.M., ASSMANN K.J.M. & KOENE R.A.P. (1989) Antiglomerular basement membrane nephritis in Beige mice. Deficiency of leukocytic neutral proteinases prevents the induction of albuminuria in the heterologous phase. *J. Exp. Med.* 169, 1435–1448.

SILVA F.G., HOYER J.R. & PIRANI C.L. (1984) Sequential studies of glomerular crescent formation in rats with antiglomerular basement membrane-induced glomerulonephritis and the role of coagulation factors. *Lab. Invest* 51, 404–415.

STERZEL R.B. & PABST R. (1982) The temporal relationship between glomerular cell proliferation and monocyte infiltration in experimental glomerulonephritis. *Virchows Arch. Cell. Pathol.* 38, 337–350.

WHEELER J., SIMPSON, J. & MORLEY A.R. (1988) Routine and rapid enzyme linked immunosorbent assays for circulating anti-glomerular basement membrane antibodies. *J. Clin. Pathol.* 41, 163–170.

ZOLLINGER H.U. & MIHATSCH M.J. (1978) General aspects of glomerulonephritis. In *Renal Pathology in Biopsy.* First edition. Eds H.U. Zollinger & M.J. Mihatsch. Berlin, New York: Springer-Verlag. pp. 182–183.